

Conference materials
UDC 538.958; 538.975
DOI: <https://doi.org/10.18721/JPM.173.106>

Photoluminescence of self-induced InAs nanowires diluted with nitrogen

M.S. Ruzhevich¹ ✉, K.D. Mynbaev², N.L. Bazhenov², A.K. Kaveev²,
A.V. Pavlov³, V.V. Fedorov^{3,4}, I.S. Mukhin³

¹ITMO University, St. Petersburg, Russia;

²Ioffe Institute, St. Petersburg, Russia;

³Peter the Great St. Petersburg Polytechnic University, St. Petersburg, Russia;

⁴Alferov University, St. Petersburg, Russia

✉ max.ruzhevich@niuitmo.ru

Abstract. Photoluminescence of arrays of self-induced nanowires consisting of pure InAs and of InAs diluted with nitrogen was studied in the 4.2–300 K temperature range. Formation of the hexagonal wurtzite (nanowires) and cubic sphalerite (mostly parasitic islands) crystal structure modifications was observed on a Si substrate used for the growth of the nanowires. A decrease in the band gap of both crystalline phases due to the introduction of nitrogen was established.

Keywords: InAs, nanowires, photoluminescence, crystal structure

Funding: This study was funded by the Russian Scientific Foundation (RSF project [22-19-00494]) for epitaxial growth of the nanowires.

Citation: Ruzhevich M.S., Mynbaev K.D., Bazhenov N.L., Kaveev A.K., Pavlov A.V., Fedorov V.V., Mukhin I.S., Photoluminescence of self-induced InAs nanowires diluted with nitrogen, St. Petersburg State Polytechnical University Journal. Physics and Mathematics. 17 (3.1) (2024) 34–37. DOI: <https://doi.org/10.18721/JPM.173.106>

This is an open access article under the CC BY-NC 4.0 license (<https://creativecommons.org/licenses/by-nc/4.0/>)

Материалы конференции
УДК 538.958; 538.975
DOI: <https://doi.org/10.18721/JPM.173.106>

Фотолюминесценция самоиндуцированных нитевидных нанокристаллов InAs, разбавленных азотом

М.С. Ружеви́ч¹ ✉, К.Д. Мынбаев², Н.Л. Баженов², А.К. Кавеев²,
А.В. Павлов³, В.В. Федоров^{3,4}, И.С. Мухин³

¹Университет ИТМО, Санкт-Петербург, Россия;

²Физико-технический институт им. А.Ф. Иоффе РАН, Санкт-Петербург, Россия;

³Санкт-Петербургский политехнический университет Петра Великого, Санкт-Петербург, Россия;

⁴Академический университет им. Ж.И. Алфёрова РАН, Санкт-Петербург, Россия

✉ max.ruzhevich@niuitmo.ru

Аннотация. В интервале температур 4,2–300 К исследована фотолюминесценция массивов самоиндуцированных нитевидных нанокристаллов из чистого InAs и InAs, разбавленного азотом. Наблюдалось формирование как гексагональной типа вюрцита (нитевидные нанокристаллы), так и кубической типа сфалерита (преимущественно паразитные островки) фаз кристаллической структуры материала на подложке Si,



использовавшейся для роста нанокристаллов. Установлено уменьшение ширины запрещенной зоны обеих кристаллических фаз при введении в материал азота.

Ключевые слова: InAs, нитевидные нанокристаллы, фотолюминесценция, кристаллическая структура

Финансирование: Работа поддержана грантом РФФИ [22-19-00494] в части эпитаксиального роста нанокристаллов.

Ссылка при цитировании: Ружевич М.С., Мынбаев К.Д., Баженов Н.Л., Кавеев А.К., Павлов А.В., Федоров В.В., Мухин И.С. Фотолюминесценция самоиндуцированных нитевидных нанокристаллов InAs, разбавленных азотом // Научно-технические ведомости СПбГПУ. Физико-математические науки. 2024. Т. 17. № 3.1. С. 34–37. DOI: <https://doi.org/10.18721/JPM.173.106>

Статья открытого доступа, распространяемая по лицензии CC BY-NC 4.0 (<https://creativecommons.org/licenses/by-nc/4.0/>)

Introduction

InAs compound semiconductor has a direct band gap and high electron mobility, and is widely used in infrared (IR) optoelectronics. The bulk InAs material has a cubic crystal lattice of the sphalerite (zinc blende, ZB) type with a band gap $E_g \sim 0.35$ eV at the temperature $T = 300$ K. Recently, interest has been growing in InAs-based nanowires (NWs); these can be used for the fabrication of photodetectors and emitters operating in the mid-IR spectral region (wavelength $\lambda = 3\text{--}6$ μm) [1–3]. The transition to NW geometry provides an efficient method for electrical and optical confinement, which can improve the efficiency of photo- and optoelectronic devices. However, the growth of low-dimensional InAs structures allows for the formation of both cubic ZB and hexagonal wurtzite (WZ) type structures [4], with E_g of the latter being ~ 0.4 eV at 300 K. In this work, we studied the influence of the morphology and crystal structure modifications on the InAs NW photoluminescence (PL) spectra. In addition, we used the PL method to study the nitrogen dilution in NWs. Introduction of nitrogen can reduce optical E_g , and thus, extend the working range of the devices to longer wavelengths. This effect is believed to originate in the changes of electronic structure of the material through the interaction between localized N levels and the InAs band states [5].

Materials and Methods

Arrays of NWs (120–150 nm in diameter and 1–2.5 μm in height) made of pure InAs and InAs diluted with nitrogen (InAsN) were grown by plasma-assisted molecular beam epitaxy (PA-MBE) using a Veeco GEN III MBE system on Si(111) substrates using the method described elsewhere [6]. With the method, NW formation occurs without the use of third-party catalysts; it proceeds in a self-induced mode at pinhole defects formed in the SiO_x layer under high temperature annealing performed after wet substrate oxidation. According to scanning electron microscopy studies, besides NWs, additional parasitic islands were formed on the SiO_x surface outside of the pinhole defects due to the tendency of nitrogen to react with SiO_x .

PL spectra were recorded in the $T = 4.2\text{--}300$ K temperature range using MDR-23 grating monochromator and excitation by a pulsed (1 kHz, 2 μs) semiconductor laser with $\lambda = 1.03$ μm . PL signal was detected with a lock-in amplifier using a cooled InSb photodiode.

Results and Discussion

Structural studies with X-ray diffractometry with reciprocal space mapping (XRD-RSM) and transmission electron microscopy showed the domination of the wurtzite structure in the NWs with clear presence of numerous stacking faults (SFs) along the [0001] growth direction.

PL spectra of the NWs recorded at low temperatures (not shown) contained two bands. At $T = 4.2$ K these PL bands peaked at energies ~ 413 meV and ~ 456 meV for a pure InAs sample, and ~ 400 meV and ~ 443 meV for an InAsN sample, respectively. The full-widths at half maxima (FWHM) of the high-energy (HE) peaks were ~ 37 meV for the InAs sample and ~ 45 meV for

the InAsN sample. For the low-energy (LE) peaks, the FWHMs equaled ~ 38 meV and ~ 29 meV, respectively. At $T = 274$ K, the FWHM of the HE peaks equaled ~ 85 meV for the InAs sample and ~ 51 meV for the InAsN sample. Comparison of the PL and XRD-RSM data suggested that the high-intensity HE peaks originated in the NWs with the WZ structure, while the less intense LE peaks were from the parasitic islands with the ZB structure. For the InAsN sample, a ~ 13 meV shift of the PL spectrum to longer wavelengths relative to that of the pure InAs sample was observed for both PL peaks.

Figure 1 shows temperature dependences of the PL peak energy position E_{PL} for the studied samples. As can be seen in Fig. 1, *a*, the $E_{\text{PL}}(T)$ dependence for the LE peak from the sample with NWs made of InAs (symbols 1) is very similar to that for the interband transitions in a commercially available ('MeGa SM') bulk (100)InAs sample; the latter dependence was recorded under similar conditions using the same experimental setup (symbols 4). Both these dependences agree very well with the $E_g(T)$ curve calculated for ZB InAs (curve 3). The LE peaks were observed in the spectra up to $T = 125$ K for the sample with NWs made of InAs (Fig. 1, *a*) and up to $T = 50$ K for the sample with NWs made of InAsN (Fig. 1, *b*). HE peaks (symbols 2) showed no pronounced $E_{\text{PL}}(T)$ dependence up to about 50 K. With temperature increasing further, the slope of $E_{\text{PL}}(T)$ dependence for these peaks approached that of the $E_g(T)$ dependence for InAs. At $T = 4.2$ K, the E_{PL} for the HE peak for InAs NWs (~ 456 meV) was smaller than the known (both from calculations and experiments, see, e.g., refs. [6, 7]) band gap of WZ InAs (~ 477 meV). This can be explained by the above-mentioned presence of SFs, as those lead to a red-shift of the PL peak compared to the calculated WZ band gap value [6].

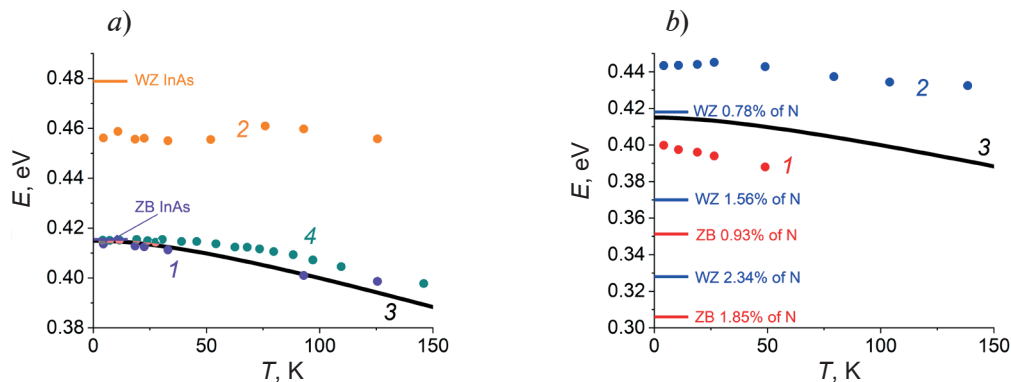


Fig. 1. Temperature dependences of the energy: of LE (1) and HE (2) PL peaks for the sample with InAs NWs (*a*) and for the sample with InAsN NWs (*b*). Solid curves 3 show calculated $E_g(T)$ dependence for ZB InAs. Dots (4) show interband PL peaks for bulk InAs (*a*). Dashes show calculated E_g values for WZ and ZB InAs (*a*) and WZ and ZB InAsN (*b*)

To estimate the amount of nitrogen incorporated in the material, WZ InAs and InAsN band structures were calculated using density functional theory (DFT) with GPAW software package [8]. A quasi-random structure (SQS) approach [9], which allows for emulating a random distribution of impurities in semiconductor alloys, was used to find the dependence of the E_g of InAsN on nitrogen concentration. The calculations were performed for two SQS constructed from the WZ InAs unit cell, with 192 and 256 atoms, corresponding to $4 \times 4 \times 3$ and $4 \times 4 \times 4$ supercells, respectively, and for one SQS constructed from ZB InAs cell with 216 atoms, corresponding to a $3 \times 3 \times 3$ supercell. Dashes in Fig. 1, *b* show the results of the DFT calculations for InAsN with various nitrogen concentrations. As can be seen, the band gap energy calculated for these concentrations appear to be significantly smaller than the energy of PL peaks observed in the experiment. Thus, to assess the actual amount of nitrogen in the material, a linear approximation for the dependence of calculated E_g on nitrogen concentration (in %) was used. For ZB InAsN structure, this approximation yielded -55 meV/% slope and the amount of nitrogen in the parasitic islands in the studied sample was estimated as 0.5%. For WZ InAsN structure, at low nitrogen concentrations (up to 1%), the calculated slope appeared to be steeper (-77 meV/%); also, the effect of the SFs, which reduced HE E_{PL} in the pure InAs NWs, had to be considered. The resulting amount of nitrogen in the material constituting NWs made of InAsN was estimated to be 0.7%.



Conclusion

In conclusion, we have studied photoluminescence of arrays of self-induced NWs grown by PA-MBE on Si substrates and consisting of pure InAs and InAs diluted with nitrogen. In the PL spectra, we observed optical transitions in both the NWs with the WZ structure and parasitic islands with the ZB-type structure, the latter being formed as a by-product of the growth. Introduction of nitrogen lead to the red shift of the PL response from both the NWs and the islands by ~ 13 meV. On the basis of this data, the nitrogen concentration in the InAsN material was assessed as 0.5–0.7%.

REFERENCES

1. **Chen H., Li J., Cao S., Deng W., Zhang Y.**, InAs nanowire visible-infrared detector photoresponse engineering, *Infrared Physics & Technology*. 133 (2023) 104785.
2. **Xu T., Wang H., Chen X., Luo M., Zhang L., Wang Y., Chen F., Shan C., Yu C.**, Recent progress on infrared photodetectors based on InAs and InAsSb nanowires, *Nanotechnology*. 31 (2020) 294004.
3. **Alhodaib A., Noori Y., Krier A., Marshall A.R.J.**, Nanowires for Room-Temperature Mid-Infrared Emission, Chapter 4 in: *Nanowires – Synthesis, Properties and Applications*. IntechOpen. 2019. Available at: <http://dx.doi.org/10.5772/intechopen.79463>. Accessed May 24, 2024.
4. **Dick K. A., Thelander C., Samuelson L., Caroff P.**, Crystal phase engineering in single InAs nanowires, *Nano Letters*. 10 (9) (2010) 3494–3499.
5. **Wu J., Shan W., Walukiewicz W.**, Band anticrossing in highly mismatched III-V semiconductor alloys, *Semiconductor Science and Technology*. 17 (8) (2002) 860–869.
6. **Fedorov V., Vinnichenko M., Ustimenko R., Kirilenko D., Pirogov E., Pavlov A., Polozkov R., Sharov V., Kaveev A., Miniv D., Dvoretckiaia L., Firsov D., Mozharov A., Mukhin I.**, Non-Uniformly Strained Core–Shell InAs/InP Nanowires for Mid-Infrared Photonic Applications, *ACS Applied Nano Materials*. 6 (7) (2023) 5460–5468.
7. **Rota M.B., Ameruddin A.S., Fonseka H.A., Gao Q., Mura F., Polimeni A., Miriametro A., Tan H.H., Jagadish C., Capizzi M.**, Bandgap Energy of Wurtzite InAs Nanowires, *Nano Letters*. 16 (8) (2016) 5197–5203.
8. **Enkovaara J., Rostgaard C., Mortensen J.J., et al.**, Electronic Structure Calculations with GPAW: A Real-Space Implementation of the Projector Augmented-Wave Method, *Journal of Physics Condensed Matter*. 22 (25) (2010) 253202.
9. **Zunger A., Wei S.-H., Ferreira L.G., Bernard J.E.**, Special Quasirandom Structures, *Physical Review Letters*. 65 (3) (1990) 353–356.

THE AUTHORS

RUZHEVICH Maxim S.
max.ruzhevich@niuitmo.ru
ORCID: 0000-0002-4513-6345

MYNBAEV Karim D.
mynkad@mail.ioffe.ru
ORCID: 0000-0002-9853-8874

BAZHENOV Nicolay L.
bazhnil.ivom@mail.ioffe.ru
ORCID: 0000-0002-3019-2280

KAVEEV Andrey K.
kaveev@mail.ioffe.ru

PAVLOV Alexander V.
a.pavlov@physics.spbstu.ru

FEDOROV Vladimir V.
fedorov_vv@spbstu.ru
ORCID: 0000-0001-5547-9387

MUKHIN Ivan S.
imukhin@yandex.ru

Received 10.07.2024. Approved after reviewing 23.07.2024. Accepted 23.07.2024.